MHD issues in Tore Supra steady-state fully non-inductive scenario

P Maget 1), F Imbeaux 1), G Giruzzi 1), V S Udintsev 2), G T A Huysmans 1), H Lütjens 3), J-L Ségui 1), M Goniche 1), Ph Moreau 1), R Sabot 1), X Garbet 1)
1) *Association Euratom-CEA, CEA/DSM/DRFC, Centre de Cadarache, 13108 S^t-Paul-lez-Durance, France*
2) *Association Euratom-Confédération Suisse, CRPP/SB/EPFL, Station 13, CH-1015 Lausanne, Switzerland*
3) *Centre de Physique Théorique, Ecole Polytechnique, Route de Saclay, 91128 PALAISEAU Cedex, France*

e-mail contact of main author: patrick.maget@cea.fr

Abstract Fully non-inductive tokamak plasma discharges are attractive for a fusion reactor, and the understanding of their MHD limitations beyond the linear stability analysis is therefore essential. Specific features of the non-inductive scheme are due to the enhanced impact of non-linear effects: one is due to the bootstrap current, and the other is linked to the intrinsic physics of plasma current generation by the external system used. In the Tore Supra tokamak, a Lower Hybrid wave launcher provides the external source (≈85% of the total plasma current), which has non-linear dependences on the plasma current and electron temperature profiles [1]. Such complex interplay is presumably the cause of spontaneous temperature oscillations that are sometimes observed [2]. But it can also cause the plasma to enter a regime with permanent MHD activity (the so-called MHD regime [3]), after the triggering of a double-tearing mode. We report observations and interpretations of MHD modes in such non-inductive discharges, with particular emphasis on their impact on the global equilibrium. We first present numerical simulations of the impact of double-tearing modes, which in experiments trigger the MHD regime. Then we report observation of MHD modes in the Oscillating regimes, at the edge of MHD unstable domain. Finally, we summarize the operational constraints to avoid the MHD regime, from the initial ohmic phase to the non-inductive phase. This study provides a better understanding of MHD limits in non-inductive discharges.

1 The double-tearing mode and its non-linear impact: experiment and simulations

The double-tearing mode (DTM) is known to cause off-axis relaxation of the plasma pressure [4, 5]. On Tore Supra, this mode produces various regimes, from the benign off-axis crash to crashes affecting the whole plasma core, and the more problematic MHD regime which in addition involves outer resonant surfaces, degrades the current drive efficiency and generates important losses of fast electrons that can damage the plasma facing components (fig. 1). We show in fig. 2 two different consequences of a DTM in a typical non-inductive discharge where most of the plasma current is provided by Lower Hybrid (LH) waves.

We have studied the DTM from a typical non-inductive pulse of Tore Supra (#33986 at $t = 26s$, $q(0) = 2.5$ and $q_{min} = 1.87$ at $r/a = 0.23$) with the code XTOR [6], which solves the evolution of the magnetic field, the velocity and the pressure (including parallel and perpendicular transport) in a fully non-inductive scheme, i.e. a source term representing non-inductive current drive $\mathbf{J_{cd}} = (\mathbf{J} - \mathbf{J_{boot}})|_{(t=0)}$ is imposed. The magnetic equilibrium is obtained from a current diffusion simulation with the CRONOS code [7], using Hard X-ray tomography for determining the LH current profile [8] and the NCLASS module [9] for the bootstrap current contribution. Because the experimental Lundquist number ($S = \tau_R/\tau_A$) is too large to be used in the simulations, we keep the ratio of energy confinement time to current diffusion time equal to its experimental value, i.e. $S\chi_\perp = (S\chi_\perp)_{exp} \sim 100$. This is equivalent to having the correct ratio of the Prandtl ($\nu/\chi_\perp$) to the magnetic Prandtl (ν/η) numbers. We also take $\chi_\parallel/\chi_\perp = 10^8$, $\nu/\eta = 1$, and $S = 5.10^6$.

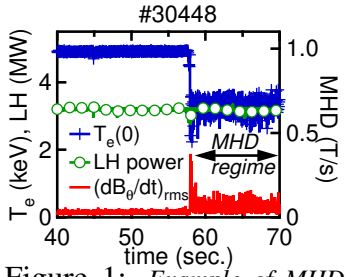

Figure 1: *Example of MHD regime.*

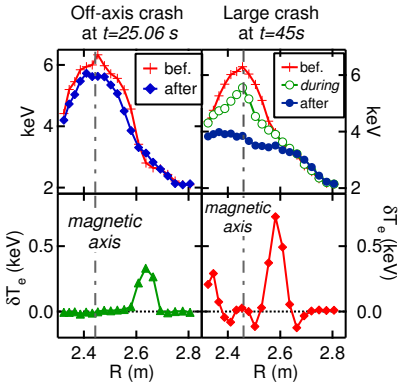

Figure 2: *#33986: Off-axis and global T_e-crashes (top) and radial structure of the MHD precursor (bottom).*

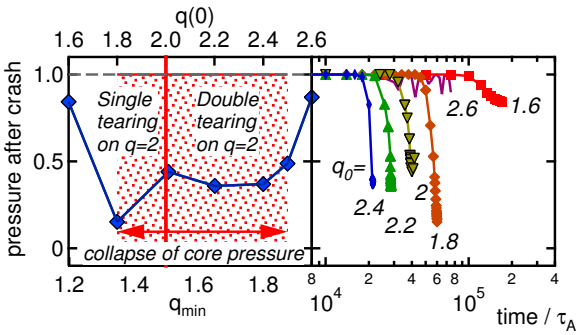

Figure 3: *Amplitude of pressure crash as a function of q_{min} and $q(0)$ (left) and time trace of core pressure (right).*

Simulations have first been run without the bootstrap current. The total plasma current is rescaled (keeping pressure and current profiles constant) so as to cover a range of $q(0)$ around 2, from the single tearing mode case ($q(0) = 1.6$) to the DTM with close resonant surfaces ($q(0) = 2.6$ with $q_{min} = 1.95$). We find the existence of a critical range around $q(0) = 2$ ($q(0) \in [1.8, 2.5]$) for which MHD modes produce a collapse of the core pressure (fig. 3), similar to experimental observations (fig.2, right). The core pressure is then reduced by 83% to 50% at the crash, while the reduction is less that 15% outside this critical range: for $q(0) = 1.6$, the single tearing saturates, and for $q(0) = 2.6$ the DTM has minor impact on the plasma confinement, as observed in fig.2 left. The collapse of the core pressure is due to the propagation of the magnetic perturbation through the region of

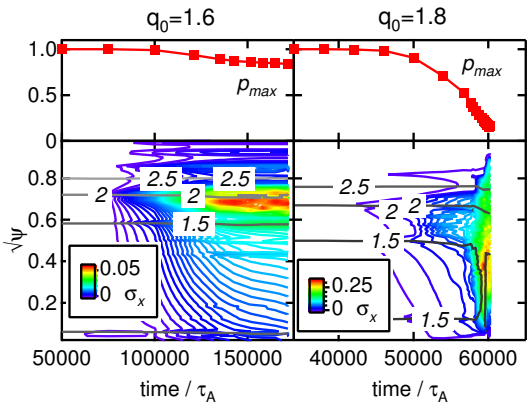

Figure 4: *Evolution of p_{max} (top) and σ_x (standard deviation of field lines) superimposed to the safety factor iso-contour (bottom) for cases $q(0) = 1.6$ (left) and $q(0) = 1.8$ (right).*

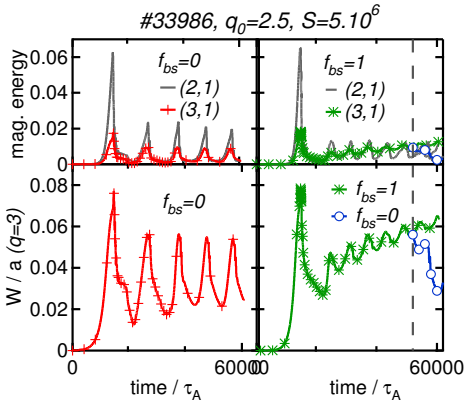

Figure 5: *DTM evolution without (left) and with (right) the bootstrap current contribution: magnetic energies (top) and island width on $q = 3$ (bottom).*

double-resonant modes with $n = 1$ or 2. This is illustrated for the single tearing case in fig. 4. The presence of a double-resonant configuration with low toroidal wave numbers ($n = 1$ or 2) is therefore detrimental.

We have investigated the effect of a finite bootstrap current (about 17% of the total plasma current in the present case) on the non-linear evolution of the DTM. We have run the case $q(0) = 2.5$ with ($f_{bs} = 1$) and without ($f_{bs} = 0$) the bootstrap current contribution (fig. 5). When the bootstrap is not taken into account, the magnetic energy of $m = 2$ and $m = 3$ components of the $n = 1$ mode are comparable. When the bootstrap current is taken into account, a destabilizing helical current perturbation is added on $q = 3$, and the $m = 3$ component increases above the $m = 2$ component. When f_{bs} is set to zero during the $m = 3$ mode growth, the $m = 3$ component immediately decays, showing that the drive for the island on $q = 3$ is the perturbed bootstrap current (this is the Neoclassical Tearing Modes (NTM) drive [10]). As for the internal kink mode, the full reconnection of a DTM is therefore a potential threat for the formation of large islands. Such an effect could participate in triggering and sustaining the MHD regime.

2 MHD modes: a powerful diagnostic for investigating oscillating regimes

Oscillating regimes are observed in low loop voltage plasma discharges, where tearing modes are absent or of small amplitude. This corresponds to a q_{min} value outside the critical range described in previous section. Fast acquisition of the electron temperature profiles during such regimes reveals the presence of MHD modes that prove to be a powerful diagnostic of the current profile evolution. In the O-regime with moderate amplitude [2], small MHD modes are observed to evolve with the T_e oscillation. They are proba-

bly electron fishbone modes associated to a double-resonant configuration [11]: their frequency ($7 - 15kHz$) is indeed in the range of the precession frequency of barely trapped electrons produced by LH waves, and their localisation coincides with that of a DTM ($1 - 4kHz$) that sometimes appears in a neighbouring period of time or even co-exists. The fishbone-like mode is localised at the foot of the oscillating region (fig. 6), which indicates that the T_e-oscillation develops in the vicinity of a low order rational resonant surface. Also, its amplitude is maximum in the hollow of the oscillation. In presence of fast ions, TAE are also observed, with a frequency that oscillates in opposite phase with the T_e-oscillations. This is consistent with a modulation of the safety factor in the O-regime which affects the localization of the TAE: since its frequency depends on the local plasma density, it also oscillates [12].

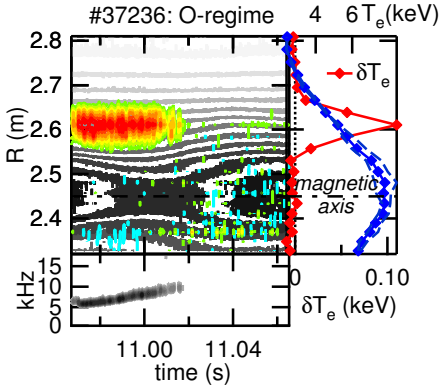

Figure 6: *O-regime: T_e (grey contours) and δT_e (colored scale) (top), δT_e, T_e^{max} and T_e^{min} profiles (right), and spectrogram (bottom).*

The O-regime can spontaneously bifurcate to a regime with much larger amplitude, where tearing modes are present. This regime is that of Giant Oscillations (GO-regime [13]). The evolution of the radial structure of δT_e during this transition is a clear illustration of the dynamics of the current profile in such regimes (fig. 7). During the slow T_e decay that initiates the GO-regime, the fishbone-like mode at $f \sim 10kHz$ co-exists with a tearing mode ($f \sim 1kHz$) whose radial structure is consistent with that of a triple tearing mode. During the T_e rise, the MHD mode has the radial structure of a double-tearing mode.

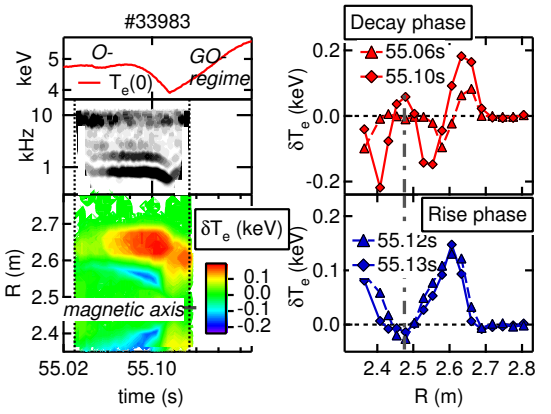

Figure 7: *$T_e(0)$ (top), spectrogram (middle) and δT_e (bottom) during O- to GO-regime transition. Right: δT_e during the decay (top) and the rise (bottom) phases.*

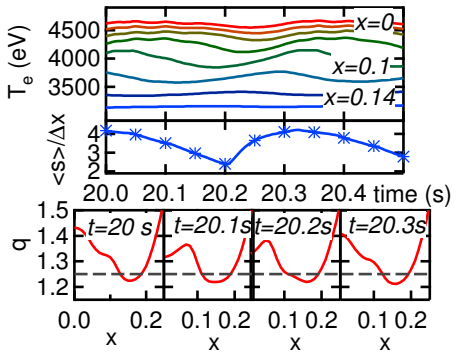

Figure 8: *Electron temperature (top), $\langle s \rangle / \Delta x \sim \beta_{crit}$ evaluated at $q = 1.25$ (middle), and $q-$profile (bottom).*

These observations have been compared to a transport simulation of the oscillating regime based on the original assumptions described in [2], with a electron diffusivity that is

reduced in presence of a negative magnetic shear and a LH absorption that depends on both T_e and the local current density profile [14]. Although this simulation does not attribute any particular role to rational safety factor surfaces, it predicts a dynamics of the current profile that is consistent with the observations reported above (fig. 8). First, the existence of a configuration with 3 resonant surfaces in the T_e decay is present in the simulation, and it evolves to a double-resonant configuration in the rise phase, in agreement with the δT_e structure observed experimentally (fig. 7). Also, if one applies the stability criterion of the ion fishbone mode to its electron equivalent, the existence of the mode in the decay phase of the oscillation is also consistent with the simulation. Indeed, the fishbone mode is unstable when the β of the hot particle population exceeds a threshold given by [15, 16]: $\beta^h_{crit} \propto \langle|s|\rangle / \Delta x$, where $\langle|s|\rangle$ is the average absolute value of the magnetic shear at the two resonant surfaces and Δx is the distance between them. Placing the resonant surface at $q = 1.25$ in the simulation gives a lower threshold in the hollow of the oscillation, in agreement with the observations (fig. 6). This consistency between the q-profile dynamics in the simulation and what is revealed by MHD modes in the experiment suggests that an ingredient linked to low order rational q-surfaces is probably missing in the present model for the O-regime. As for the issue of Internal Transport Barrier triggering [17, 18, 19], this ingredient could be related to a specific reduction of anomalous transport at rational q values with a vanishing magnetic shear [20], as supported by recent observations [21], or to an active role of MHD modes [22, 23, 24]. Finally, one can note that the GO-regime seems to exhibit a dynamics of the current profile that is similar to that of the O-regime, but with a safety factor that is lower. This triggers tearing modes and forms an intermediate stage between the O-regime and the off-axis sawtoothing regime. Actually, these 3 regimes are sometimes observed one after the other in a same discharge.

3 Safe operation diagram for non-inductive discharges: preforming and steady-state

Operating a non-inductive discharge on Tore Supra requires avoiding the triggering of the MHD regime, which severely degrades the confinement and the current drive efficiency, with potential damage to the plasma facing components. This regime is triggered during the non-inductive phase after the full reconnection of a DTM, but it can also appear very early in the plasma discharge, as soon as LH is switched on.

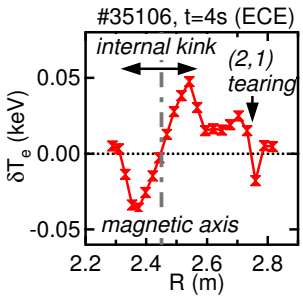

Figure 9: *δT_e in the ohmic phase.*

We first consider the triggering of MHD modes at LH start. This appears to be related to the nature of the sawtoothing regime in the ohmic phase: small sawtooth amplitude (of T_e crash) is associated to the presence of an island on $q = 2$ (fig. 9), which grows to larger size when LH is switched on: as the current profile becomes hollow, the amplitude of MHD mode increases, with important

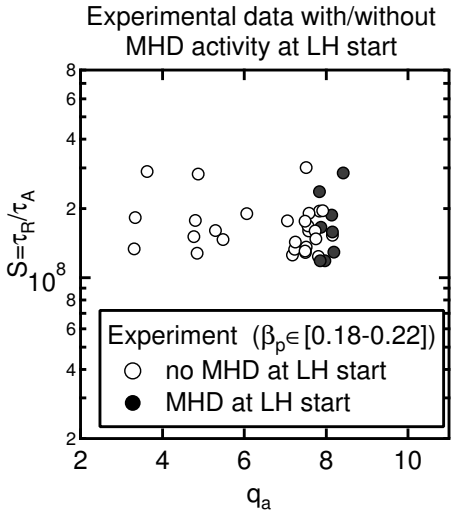

Figure 10: *Experimental points from the database with* $\beta_p \in [0.18, 0.22]$ *as a function of* S *and* q_a.

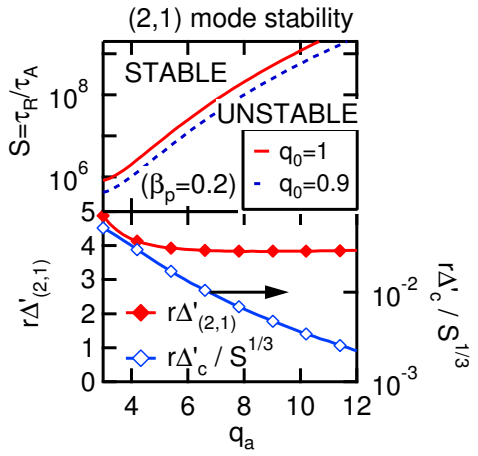

Figure 11: $\Delta'_{eff} = 0$ *as a function of* q_a *and* S *for the (2,1) mode (top);* $r\Delta'$ *and* $r\Delta'_c/S^{1/3}$ *as a function of* q_a *for* $q(0) = 1$ *(bottom).*

crashes of T_e leading eventually to the MHD regime. On a statistical basis, it appears that this situation is encountered in ohmic phases with a high edge safety factor q_a (fig. 10).

The explanation can be found in the linear stability properties of the $(m = 2, n = 1)$ mode including curvature effects: $\Delta'_{eff} = \Delta' - \Delta'_c = 0$ where Δ' is the tearing stability index in cylindrical geometry and [25]

$$r\Delta'_c = 1.54 \left[x^4 (ns)^2/(1+2q^2)\right]^{1/6} S^{1/3} D_R^{5/6}$$

with $x = r/a$ and D_R the resistive interchange parameter. A parametric study of the stability threshold ($\Delta'_{eff} = 0$) as a function of q_a and the Lundquist number S is performed for a family of current profiles $J = J_0 \left(1 - x^2\right)^{\alpha}$ and a pressure profile $p = p_0(1-x^2)^2$. The value of p_0 is such that $\beta_p = 0.2$, corresponding to the typical experimental value of Tore Supra ohmic discharges, and J_0 is such that $q(0) \sim 1$. This analysis shows that the unstable domain expands to higher S values at high q_a, due to weakening of the stabilizing curvature effect, while the tearing index varies little in the range $q_a \in [3 - 16]$ (fig. 11). Indeed, the curvature effect has a strong dependence on the $q = 2$ surface position ($r\Delta'_c \propto x^{7/3}$), and it vanishes at high q_a when $q = 2$ gets closer to the magnetic axis. This result supports the empirical recipe that is generally used for the preforming phase of non-inductive discharges in Tore Supra, which consists in operating the ohmic phase at higher plasma current (lower q_a) than the non-inductive phase.

We now address the question of the triggering of the MHD regime in the non-inductive phase, one can use a diagram where the stability limits of the double-tearing mode are drawn as a function of global variables such as the total plasma current, the magnetic field and the parallel refractive index of LH waves (which affects the radial profile of LH

absorption). The operating map needs only to localise the region where the MHD regime is triggered, which corresponds approximately to cases where MHD modes produce a global crash of the pressure. Results from the Tore Supra fully non-inductive experiments are shown in fig. 12. On the left is shown the diagram of ref. [3], where a scaling in I_p was performed on the basis of 3 experimental cases for plotting q_{min} as a function of I_p at the 3 magnetic fields investigated. The domain in (B, I_p) that have been covered by the experiments is shown ("explored"). Cases where the MHD regime is triggered are marked with a star, and this is schematically extrapolated to the whole diagram. Such a diagram is compared with a characterization of the plasma regime from a recent database of about 50 non-inductive pulses. The domains where $q_{min} \sim 2$ or $\sim 3/2$ can be inferred when the parity of MHD modes can be determined. Differences in additional plasma parameters can explain the dispersion. The domain of potential threat (MHD regime) is confirmed by this statistical approach. Such a diagram is useful for preparing and operating reliable non-inductive discharges. In addition, it allows using a procedure for anticipating the triggering of the MHD regime.

4 Conclusion

Non-inductive discharge operation in Tore Supra has revealed several specific issues linked to rational q-surfaces and MHD activity. At the edge of the MHD unstable domain, Oscillating regimes are observed, and as q_{min} is getting lower below the rational, off-axis sawteeth or a global crash are produced, with possible transition to the MHD regime. Numerical simulations with the XTOR code show that the bootstrap current perturbation after a global crash can drive a large island on $q = 3$, which could play a role in sustaining the MHD regime. From the point of view of the operational domain for getting reliable non-inductive discharges, the regions $q_{min} \lesssim 2$ and $q_{min} \lesssim 3/2$ should clearly be avoided. In between these two regions, the experimental database shows that there is a domain $q_{min} \in [\sim 1.5, \sim 1.8]$ where MHD modes have no major impact on the discharge: the record pulses in terms of duration and injected energy were indeed performed (at $B = 3.3T$) in presence of a continuous mode on $q = 3/2$. This contrasts with the pessimistic prediction from numerical simulations based on a $B = 3.8T$ pulse (see fig. 3), where the $n = 1$ mode gives rise to a global crash in a larger domain $q_{min} \in [\sim 1, \sim 2]$, due to the presence of close double-resonant surfaces at low n in this range. This discrepancy comes from the linear stability of $n = 1$ mode, which is more favourable in the experiment than deduced from the MHD model for the reconstructed equilibrium: additional physical effects in the model, and error bars in the reconstruction, may account for the difference.

Crossing experimental observations and numerical simulations has provided a better understanding of the MHD limits of the non-inductive discharges in Tore Supra. Physics issues can then be addressed for the optimisation of this scenario in terms of reliability and performance.

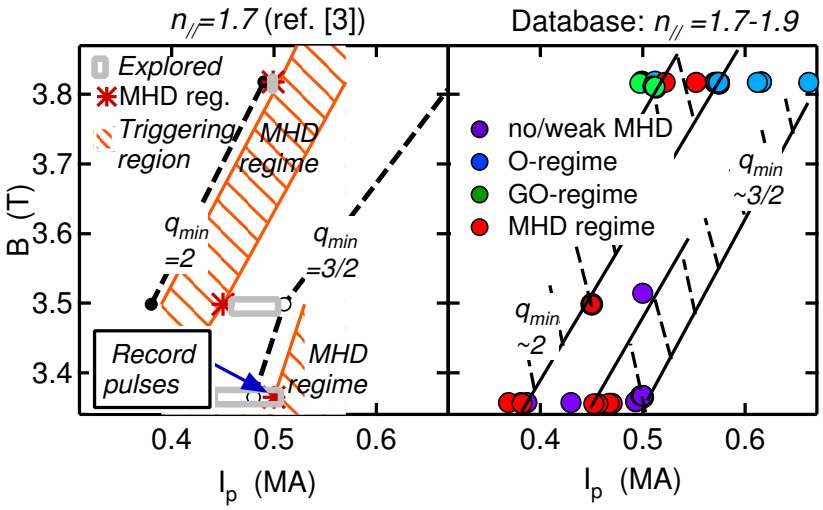

Figure 12: *Left: Diagram for safe non-inductive operation in (B, I_p) space for $n_{\|} = 1.7$: q_{min} from experimental cases at 3 values of B rescaled in I_p and schematic drawing of the region to avoid. Right: Database of plasma regimes for non-inductive pulses ($n_{\|} \in [1.7, 1.9]$).*

References

[1] PEYSSON Y. and the Tore Supra Team *Plasma Phys. Control. Fusion* **42** B87 (2000)
[2] GIRUZZI G. et al *Phys. Rev. Lett.* **91** 135001 (2003)
[3] MAGET P. et al, *Nuclear Fusion* **45**, 69 (2005)
[4] CARRERAS B. HICKS H.R. and WADDELL B.V. *Nuclear Fusion* **19** 5863 (1979)
[5] CHANG Z. et al, *Phys. Rev. Letters* **77**, 3553 (1996)
[6] LERBINGER K. and LUCIANI J.-F. *J. Comp. Phys.* **97**, 444 (1991)
[7] BASIUK V. et al *Nuclear Fus.* **43** 822 (2003)
[8] PEYSSON Y. and IMBEAUX F. *Rev. Phys. Instrum.* **70** 3987 (1999)
[9] HOULBERG W. A. et al *Phys. of Plasmas* **4** 3230 (1997)
[10] CARRERA R., HAZELTINE R.D. and KOTSCHENREUTHER M *Phys. Fluids* **29** 899 (1986)
[11] MAGET P. et al, *Nuclear Fusion* **46**, 797 (2006)
[12] UDINTSEV V S et al *Plasma Phys. Control. Fusion* **48** L33 (2006)
[13] IMBEAUX F et al *Phys. Rev. Letters* **96** 045004 (2006)
[14] IMBEAUX F et al in Fusion Energy 2004 (*Proc.* 20^{th} *Int. Conf. Villamoura, 2004*) (Vienna:IAEA) CD-ROM file EX/P6-16 and http://www-naweb.iaea.org/napc/physics/fec/fec2004/datasets/index.html

[15] HELANDER P. et al *Phys. Plasmas* **4** 2181 (1997)
[16] HUYSMANS G.T.A. et al *Nuclear Fusion* **39** 1489 (1999)
[17] ERIKSSON L.G. et al *Phys. Rev. Lett.* **88** 145001-1 (2002)
[18] BELL R.E. et al *Plasma Phys. Control. Fusion* **40** 609 (1998)
[19] JOFFRIN E. et al *Nuclear Fusion* **43** 1167 (2003)
[20] GARBET X. et al *Phys. Plasmas* **4** 1792 (2001)
[21] AUSTIN M.E. et al *Phys. of Plasmas* **13** 082502 (2006)
[22] JOFFRIN E. et al *Nuclear Fusion* **42** 235 (2002)
[23] IDA K. et al *Physical Review Letters* **88** 015002-1 (2002)
[24] GUNTER S. et al *Proc. of the 28th EPS Conference on Controlled Fusion and Plasmas Physics, Madeira* **25A** 49 (2001)
[25] GLASSER A.H. GREENE J.M. and JOHNSON J.L. *The Phys. of Fluids* **19** 567 (1976)